Semnan University

Mechanics of Advanced Composite Structures

Journal homepage: https://macs.semnan.ac.ir/

ISSN: 2423-7043

Research Article

Influence of Basalt/Carbon/Steel Fibers Addition on Flexural and Vibration Characteristics of Epoxy Granite

Deepak Ubale [a]*, Abhijeet Shah [a], Samir Kumbhar [a]

[a] *Department of Mechanical Engineering, Kasegaon Education Society's Rajarambapu Institute of Technology, affiliated to Shivaji University, Sakhrale, Maharastra, India.*

A R T I C L E I N F O

Article history:

Received: 2024-10-19
Revised: 2025-03-22
Accepted: 2025-05-12

Keywords:

Epoxy Granite;
Damping ratio;
Basalt Fibers;
Carbon Fibers;
Steel Fibers.

A B S T R A C T

Large-scale efforts have been made to produce composites for machine tool structural parts as an alternative to cast iron and steel, etc. This paper presents a comprehensive approach to investigate flexural and vibration characteristics by experimental study and its validation by the finite element analysis of epoxy granite added with different fibers. The three kinds of short fibers, viz. basalt, carbon, and steel fibers, were added separately to form three composites, such as BFREG, CFREG, and SFREG, respectively. The volume ratios of granite particles, epoxy resin, and short fibers were fixed to 75%, 20%, and 5%, respectively. The test specimens were prepared and examined in density tests, 3-point flexural tests, and vibration tests. The finite element(FE) modal analysis was performed to determine the numerical frequencies and mode shapes. The study demonstrates that the fibers used in the composites significantly influence the flexural and vibration characteristics. The BFREG and SFREG exhibit excellent flexural and vibration performances, respectively. The mean damping ratio of the SFREG is 37% and 118% greater than BFREG and CFREG, respectively. The lower standard deviations highlight the consistency of experimental results. The close agreement of experimental and numerical results validates the numerical model.

1. Introduction

Vibrations produced during the machining process have a negative effect on surface finish, dimensional accuracy, and other aspects of machining quality. Examples of structural elements that must be able to withstand the cutting forces and vibrations produced during the machining process are the bed, base, and columns of machining centers. These structural components ought to have adequate vibration damping capacity and static rigidity. The polymer concrete made of quartz and polyester resin with varying compositions was examined for damping. Compared to traditional cast iron, the damping ratio of polymer concrete with 20% polyester resin demonstrated more damping [1]. Tests on epoxy polymer plain concrete reinforced with glass and carbon fibers were conducted. A 6 mm long fiber with 1% and 2% weight was taken in 1% and 2% increments, respectively. The glass and carbon fibers were irregularly distributed throughout the polymer concrete. The results for reinforced composition demonstrated improvement in modulus and compressive strength [2]. The polymer concrete (PMC) with epoxy combinations of 15% and 20% and 50% small and 50% large granite particles by weight ratio showed the maximum compressive strength [3].

* **Corresponding author.**
E-mail address: *ubaledd@gmail.com*

Cite this article as:
Mohammadi, A. and Mahdi-Nia, M., 2026. Title of article. *Mechanics of Advanced Composite Structures*, 13(1), pp. xxx-xxx.
https://doi.org/10.22075/MACS.2025.39315.2050

The complex modulus of polymer concrete was measured and compared with grey cast iron by a method that uses hundreds of measuring points. Nelder–Mead minimization algorithm was used for curve fitting. The experimental data evidence that damping capacity was higher for polymer concrete than grey cast iron[4]. Glass fiber-reinforced polymer concrete was examined in damping experiments to determine the damping ratio. The granite ratio had a significant impact on the damping ratio; then the fiber length and flexibilizer content had a moderate impact, and lastly the glass fiber and epoxy resin had a negligible impact on damping [5]. Epoxy granite composites with varying epoxy and granite powder compositions were examined for damping ratios. The composition of 80% granite and 20% epoxy showed improved damping as compared to grey cast iron [6]. The machine construction made of carbon epoxy composite and resin concrete was created with the aim of reducing weight. Finite element analysis and vibration tests were used to establish the structures' dimensions. This new structure's results demonstrated considerable mass reduction and gain in structural stiffness [7]. The granite particle and epoxy samples were subjected to a compression test. The mixture of 20% epoxy and 50% granite particle proportion by weight yielded the highest compressive strength [8]. The specimen with 50% coarse aggregates had the maximum compressive strength and elastic modulus [9].

The compression experiments were conducted on epoxy granite with cast iron particles in weight ratios of 5, 10, and 15%. The maximum compressive strength was achieved for a 30% epoxy by weight ratio. The compressive strength rises with an increase in the amount of cast iron particles [10]. The carbon fiber-reinforced composite material milling machine model was created to conduct the experimental tests and finite element analysis. As the stiffness increased, the weight decreased with improvement in the machining performance [11]. The effects of particulate composition on damping ratio and elastic modulus were studied for machine tool applications. A quartz-filled composite (polyester 30% and particles ≤2 mm) showed significantly greater damping than cast iron and steel. To retain the same stiffness, this composite was included in a steel structure up to 75% volume. The hybrid system showed significantly improved damping with negligible reduction in stiffness and enhanced surface finish[12]. The damping ratios were investigated for granite particles of different weights. A 20% epoxy and 80% granite grit combination showed an improved damping ratio[13]. Epoxy composite beams reinforced with glass, carbon, and basalt fibers were tested to determine the damping ratio. The glass fiber epoxy laminate composite showed the highest damping ratio [14]. Fiberglass-reinforced epoxy and basalt granules containing silica particles were used to test the tensile strength. Fiberglass reinforcement showed ductile behavior. High stiffness and elongation-free breaking have been observed in specimens lacking fiberglass reinforcement [15]. Epoxy concrete that had three different-sized rubber particles added—0.5 mm for fine, 1.5 mm for medium, and 4 mm for coarse—was tested for flexural strength. Medium-sized rubber particles are advised based on test results [16].

Flexural strength tests were performed on an epoxy granite composite that had 80% granite and 20% epoxy by weight. 20.1 MPa was the maximum flexural strength measured [17]. For a composite of epoxy resin by 12% weight and crushed granite particles measuring 1.18–2.36 mm, 0.6–1.18 mm, and < 0.6 mm, the compressive strength of epoxy granite was measured. The composite material containing fine granite particles has the highest compressive strength, 18.1 MPa, according to the data [18]. A mathematical model was developed to examine the porosity effect on the mechanical properties like damping ratio and flexural strength. Theoretical porosity was estimated by using component properties and their volume fractions. Taguchi design of experiments was employed for testing, and empirical relationships were established by regression analysis[19]. Modal tests for polymer concrete with different resin contents were used to examine the impact of resin on damping. Granite epoxy specimens with a 50:25:25 granite proportion for fine, medium, and big epoxy resin were examined for damping ratio. For 20% and 25% epoxy resin, the highest damping ratios of 0.0202 and 0.015 were noted [20]. Using glue and a maximum silica sand aggregate size of 3.15 mm, test specimens of 10x25x500 mm were created. For 19% and 17% resins, the highest and lowest damping ratios were noted [21]. The performance of polymer concrete was examined by integrating the prestressed continuous carbon fiber reinforcements up to 470 MPa. Bending strength and stiffness showed improvement by 35% and 16%, respectively, with significant delayed crack initiation[22].

Composite laminates made of glass, kenaf, and hybrid skin materials were examined for their damage behavior. When it comes to energy absorption and damage area reduction, the hybrid skin structure performs better. Compared to full kenaf composites, the hybrid specimens absorb 218% more energy [27]. The flexural performance of single (SSS) and double (DSS) symmetry-broken models of star-shaped honeycomb meta-materials was investigated. The SSS design outperformed the conventional structure by around 26.8% in SEA at 40 mm deflection under flexural loads [28]. The impact of carbon nanofiber (CNF) on the thermomechanical characteristics of polymeric nanocomposites with random orientation and distribution was investigated. The transverse-aligned CNFs have no effect on residual stresses compared to a random distribution. But in the case of glass fiber(GF)/CNF/epoxy nanocomposites with 2 wt.% transverse-aligned CNFs, the reduction in residual stresses was observed to be 17% higher than their random distribution[29].

The majority of research works are focused on experimental studies of the damping capacity of granite-epoxy compositions. Limited studies have reported on the addition of cast iron particles and fibers in granite-epoxy mixtures. A thorough approach for examining flexural and damping behavior is absent. The primary goal of this work is to analyze the flexural and damping behaviors by experimental inquiry and validation simultaneously by using finite element analysis.

2. Experimental

2.1 Materials and Fabrication of Composites

First, the methodology of the study to be conducted is defined well, as shown in Figure 1. Based on the literature studied, the selection of the ingredient materials on the basis of certain properties is performed. The granite of Indian origin was selected as filler satisfying the required properties such as density, compressive and bending strengths [23]. Table 1 and 2 shows the properties of Indian granite and the volume fraction of granite particles. The waste granite pieces were manually crushed and categorized into four distinct sizes, as shown in Figure 2. The carbon and basalt fibers are added due to excellent damping properties[14]. The length of short chopped fibers is decided on the basis of the width of the test specimen(maximum 50 mm). The fibers added in the mixture are randomly dispersed and oriented. Table 3 shows the technical specifications of selected fibers. Bisphenol A type epoxy, namely "LY 556," is selected based on its properties listed in Table 4, having moderate viscosity useful to impart viscous character, playing a crucial role in damping behaviour. Figure 3 shows the LY 556 epoxy resin and Ardur 951 hardener used. The LY 556 epoxy resin and Ardur 951 hardener were utilized in a weight ratio of 10:1 as per the technical data provided by the manufacturer. The chopped fibers, epoxy resin, and granite particles were taken in the proportion shown in Figure 4. This mixture was stirred manually until a uniform, homogeneous mixture. The prepared mixture was poured into the mold cavity at a uniform rate with continuous shaking on a vibration table. The filled mold was allowed to cure at room temperature for a minimum of 24 hours. The test specimens of 50 × 50 × 300 mm are fabricated in accordance with C78/C78M of three compositions viz. Basalt fiber-reinforced epoxy granite (BFREG), Carbon fiber-reinforced epoxy granite (CFREG), and Steel fiber-reinforced epoxy granite (SFREG), as shown in Figure 5.

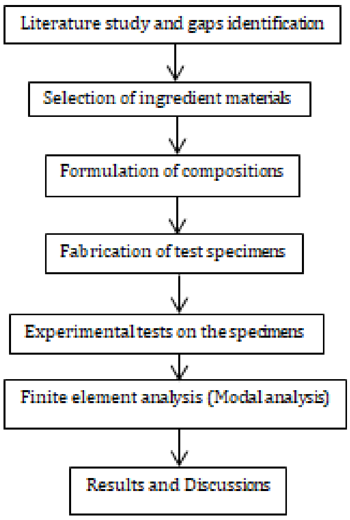

Fig.1. Methodology of study

Table 1. Properties of Indian granite

Density [Kg/m³]	Compression Strength [MPa]	Bending Strength [MPa]
2.8-3	170-190	18-22

Table 2. Volume fraction of granite particles

Particle size	<1 mm	1- 3 mm	3-5 mm	5-8 mm
Volume fraction	20	30	30	20

Table 3. Technical Specifications of fibers

Specification	Basalt fiber	Carbon fiber	Steel fiber

Diameter[micron]	20	7	600
Length(mm)	12	12	30
Density[Kg/dm3]	2.7	1.8	7.8
Modulus of Elasticity[GPa]	90-100	70-75	200-210

Table 4. Properties of araldite LY556[25]

Physical	Chemical
dimensional stability, excellent resistance to water, non-toxic, no taste	moderate viscosity and unmodified liquid epoxy resin

Fig. 2. Actual photograph of granite particle sizes and various types of fibers

Fig. 3. Actual photograph of epoxy resin (LY 556) and hardener (Aradur 951)

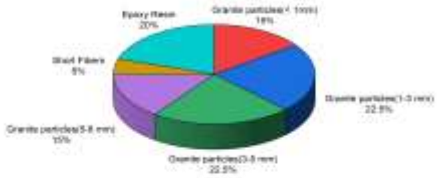

Fig. 4. Distribution of Volume fraction

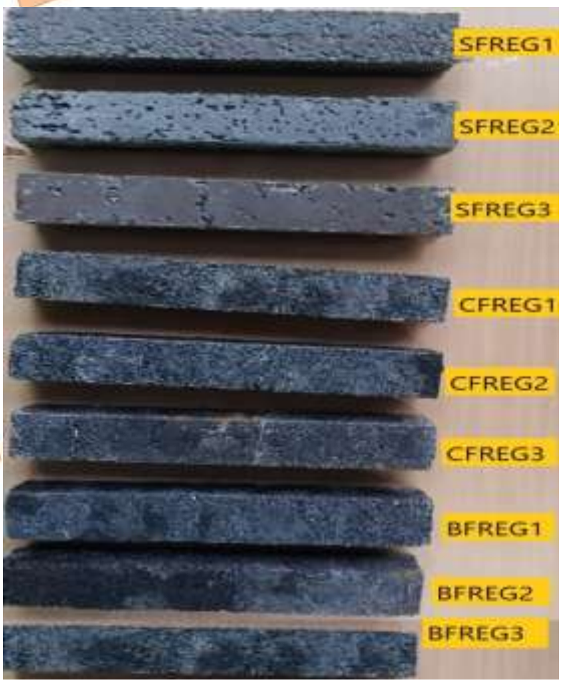

Fig. 5. Actual photograph of test specimens fabricated

2.2 Density Test

The mass density affects inertia and vibrations in terms of natural frequencies and damping. Density does not affect strength, but it affects stiffness and strength-to-weight ratio. Therefore, there is a necessity to have an optimum density for stiffness and damping trade-off. The aim of the density test is to study the effect of mass density on vibration behavior. The mass density of test specimens is determined according to ASTM C138/C138M. The mass (m) of test specimens measured in kilograms and volume (v) of the specimen in cubic meter by relation 1. Table 5 shows calculated densities of respective compositions.

$$\rho = \frac{m}{v} \qquad (1)$$

Table 5. Sample readings of mass density

Composition	Reading	Reading	Reading

	1	2	3
BFREG	2270	2313	2306
CFREG	2343	2318	2305
SFREG	2445	2486	2464

2.3 Flexural Test

Under bending vibration, the structure's flexural capacity is one of the characteristics used to measure dynamic performance. It is the ability of a structure to resist bending loads. The objective of the test is to study the relationship between the flexural behavior and damping behavior. The flexural capacity is one of the The flexural tests conducted in accordance with C78/C78M on fabricated test specimens. At the midpoint of the test specimen, as depicted in Figure 6. The transverse force is applied gradually and uniformly. The flexural strength (σ_f) is given by equation 2. Flexural tests are conducted on a computerised universal testing machine as shown in Figure 7. Table 6 shows the maximum loads taken by specimens under flexural tests and computed flexural capacities of respective specimens.

$$\sigma_f = \frac{3PL}{2bh^2} \quad (2)$$

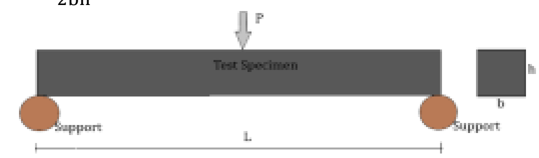

Fig.6. Schematic diagram of Three-point flexural test

Fig. 7. Actual photograph of Three-point flexural test

Table 6. Readings of flexural test and values of flexural capacities

Specimen No.	Maximum Load [kN]	Flexural Strength [MPa]
BFREG1	4.4	14.78
BFREG2	4.9	16.46
BFREG3	4.6	15.46
CFREG1	4.1	13.78
CFREG2	3.3	11.09
CFREG3	3.4	11.42
SFREG1	3.7	12.43
SFREG2	3.4	11.42
SFREG3	3.1	10.42

2.4 Vibration Test

The main aim to conduct vibration test is to measure damping capacity and natural frequencies. Figure 8 illustrates the vibration test setup used to calculate the damping ratios of fiber-added epoxy granite. The flexural test specimens were tested for vibration tests before flexural tests. The damping ratios were measured on the test specimens under free-fix conditions. In order to record the responses under damped free vibrations, an accelerometer was installed. The tests were conducted as shown in Figure 8 using a tri-axial CCLD piezoelectric accelerometer with a sensitivity of 9.507 mV/g. The Pulse Labshop data acquisition unit interfaced with the computer, accelerometer, and impact hammer, as shown in Figure 9.

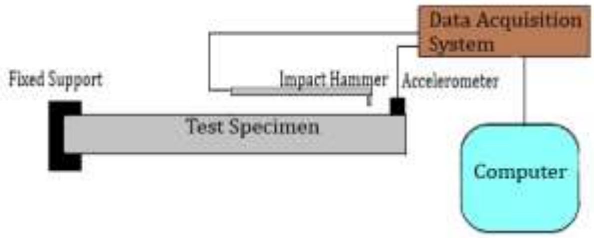

Fig. 8. Schematic diagram of vibration damping measuring setup

Fig. 9. Actual photograph of Vibration damping measuring tests

The damping ratio is determined by the half-power bandwidth method. The bandwidth is normalized across the peak response at the amplitude of 0.707 of maximum amplitude (A_{max}) as shown in Figure 10. Equation 3 is used to determine the damping ratio(ξ) based on peak frequency(f_n), maximum frequency (f_2) and minimum frequency (f_1) normalized acorss peak response.

$$\xi = \frac{f_2 - f_1}{2f_n} \tag{3}$$

The impact test by hammer was repeated till the frequency response curves were consistent with previous responses. Figure 11 shows samples of consistent frequency responses recorded. Table 7 shows frequencies and corresponding damping ratios computed at peak responses observed by half power band width method.

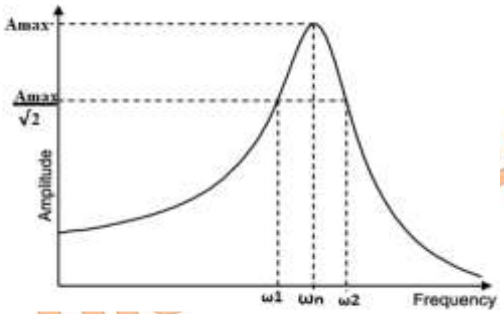

Fig. 10. Image of bandwidth normalized across the peak response

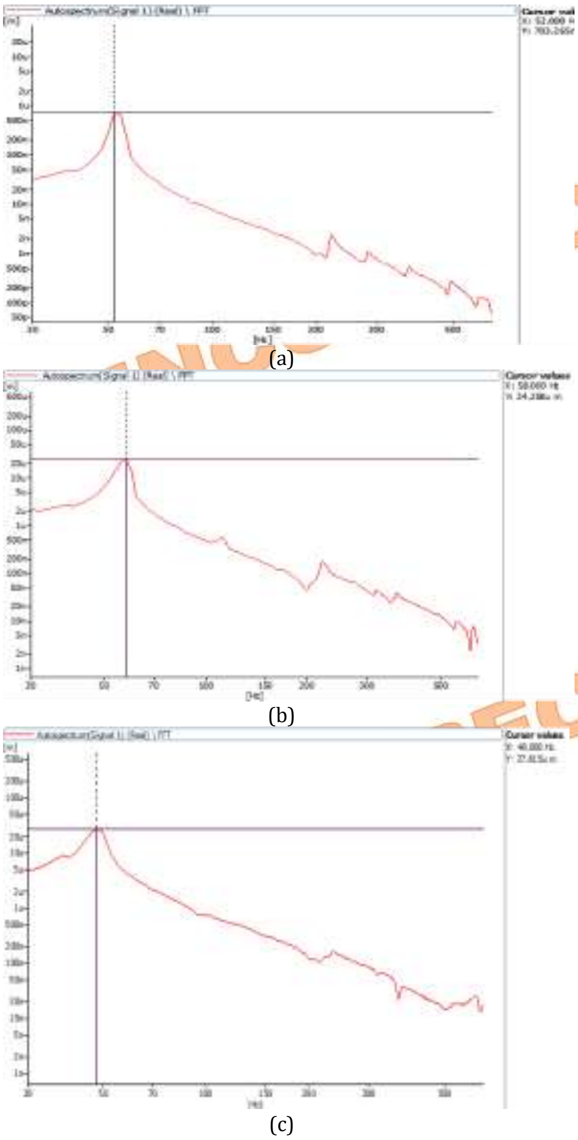

Fig. 11. Samples of recorded frequency responses of (a) BFREG, (b) CFREG and (c) SFREG

Table 7. Damping ratios at corresponding frequencies

BFREG	CFREG	SFREG
At 52 Hz, ξ = 0.039	At 58 Hz, ξ = 0.026	At 48 Hz, ξ = 0.052
At 282 Hz, ξ = 0.049	At 222 Hz, ξ = 0.029	At 328 Hz, ξ = 0.053
At 514 Hz, ξ = 0.0156	At 628 Hz, ξ = 0.012	At 618 Hz, ξ = 0.04

3. Modal Analysis

The main aim of modal analysis is to determine natural frequencies and mode shapes, and to compare numerical frequencies with experimental frequncies. In order to determine the numerical frequencies of the beam, the modal analysis was carried out in Ansys (2023/R1) software. The 3D model of 50 × 50 × 300 mm was created, and new materials were added by importing the material data, including density, Poisson's ratio, and elastic modulus. The model in modal analysis is subjected to free-fixed boundary conditions.

Table 8 shows the values of input parameters like density, modulus of elasticity, and Poisson's ratio of various compositions used in modal analysis. The frequencies and mode shapes at different modes are obtained by performing the modal analysis, as shown in Figure 12.

Table 8. Input parameter values for modal analysis

Parameter	Value
Number of Nodes	26213
Number of Elements	5600
Density of BFERG	2296 Kg/m³
Density of CFERG	2322 Kg/m³
Density of SFERG	2465 Kg/m³
Modulus of Elasticity of BFERG	1.1 GPa
Modulus of Elasticity of CFERG	1 GPa
Modulus of Elasticity of SFERG	1.25 GPa
Poisson's Ratio of BFREG	0.265
Poisson's Ratio of CFREG	0.25
Poisson's Ratio of SFREG	0.26

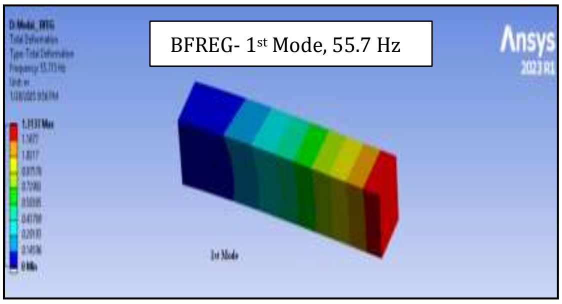

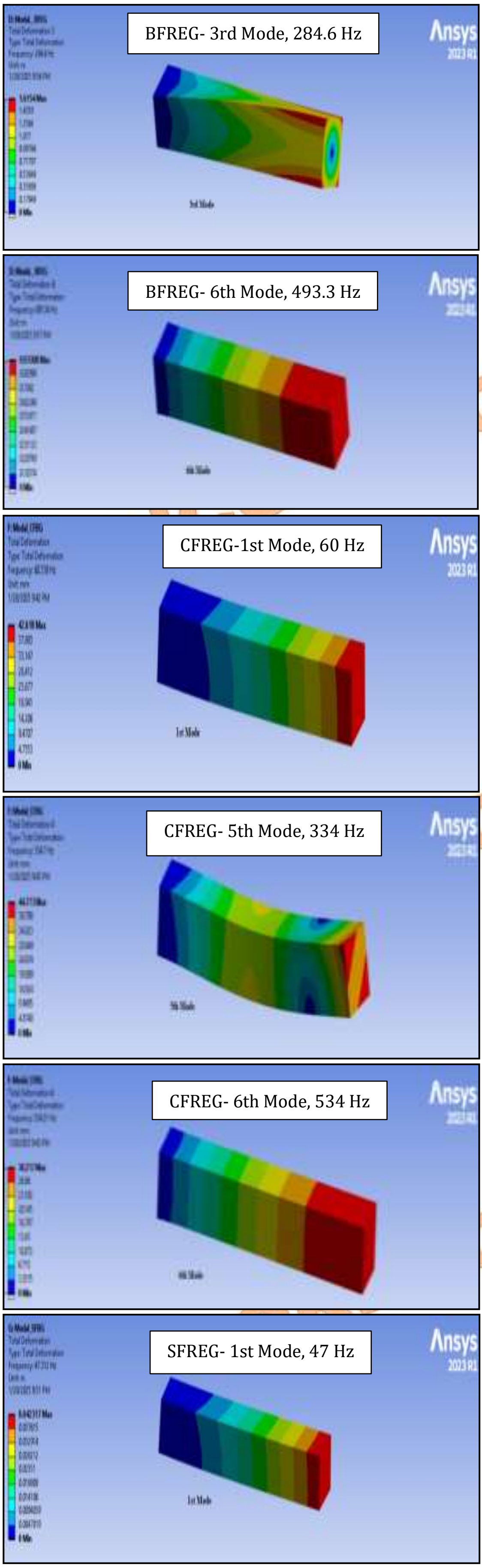

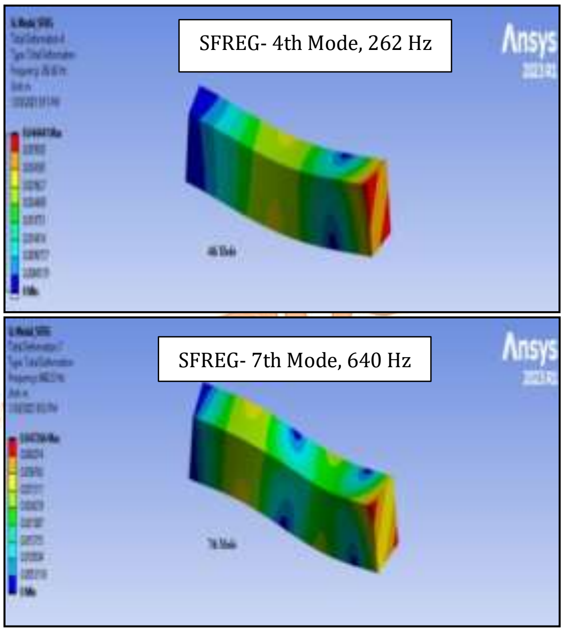

Fig. 12. Sample photograph of modal analysis performed

4. Results and Discussions

Each test specimen of composites was first tested in a density test, then in the vibration test, and finally in the flexural test. If any deviation in computed values is observed beyond ±15% of the mean values, then that particular value is omitted. The respective tests were repeated to ensure consistency. In the density test, the mass density and the mean mass density are computed. In the vibration test, the frequency response curve of each specimen is observed, and the vibration test procedure is repeated until the response repeats itself nearly the same as the previous response. The final response curves of each specimen are recorded in the software. In the flexural test, load versus displacement is recorded till first evidence of failure is observed. The flexural capacity on the basis of maximum load is computed, and then the mean flexural capacity. The mean and standard deviations are computed to ensure the consistency of results.

4.1 Fibers' Influence on the Density

Table 9 shows the computed mean mass densities and standard deviation of composites examined. The lower value of standard deviation of all composites shows that the computed mass density values are closer to mean values. The lowest standard deviation of CFREG indicates that there is uniformity in processing, which gives a uniformly distributed mix. The BFREG shows a little more standard deviation, which indicates that there is slight variability exists in composition.

Table 9. Mean Density and Standard Deviations

Composition	Mean Density	Stdadard Deviation
BFREG	2296	22.86
CFREG	2322	19.67
SFREG	2465	20.52

4.2 Fibers' Influence on the Flexural Capacities

Table 10 shows the computed mean and standard deviation of the flexural capacities of fibers-added epoxy granites. The BFREG shows the lowest deviation among all compositions. This indicates strong bonding and consolidation between the matrix and uniformly distributed fibers. It also indicates a well-structured and homogeneous composition. Whereas CFREG shows higher standard deviation, indicating structural inhomogeneity due to weak interfacial bonding despite the high stiffness of carbon fibers. The SFREG shows comparatively lower flexural capacities than others due to dispersion issues.

Table 10. Mean flexural capacity and Standard Deviations

Composition	Mean Flexural capacity [MPa]	Stdadard Deviation
BFREG	15.57	0.85
CFREG	12.10	1.45
SFREG	11.42	1.01

Figure 13 shows a few samples of load versus displacement plots. The BFREG exhibits excellent flexural performance with higher load-carrying capacity and stable crack propagation due to excellent bonding between fibers and matrix. The failure modes of composites are shown in Figure 14. The CFREG shows moderate stiffness but undergoes a brittle type of failure. The SFREG shows ductile behavior, indicating improved energy absorption by fiber bridging mechanisms.

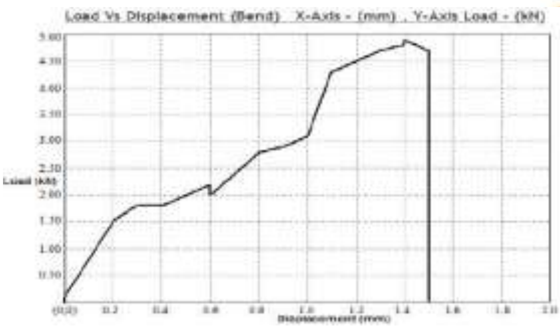

(a)

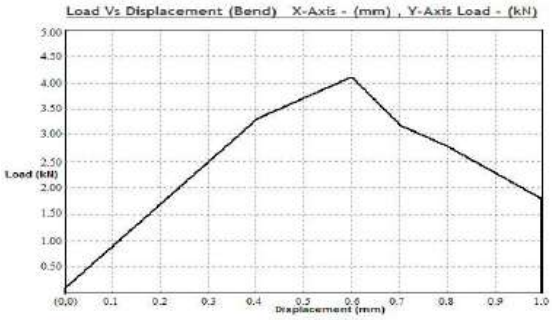

(b)

(c)

Fig. 13. Samples of load vs. Displacement plot of (a) BFREG, (b) CFREG, and (c) SFREG

BFREG

CFREG

SFREG

Fig. 14. Crack propagation and failure modes of composites

4.3 Fibers' Influence on the Frequencies

Table 11 summarizes the experimental frequencies and the numerical frequencies at various modes. It shows that natural frequencies vary significantly with fiber type. The SFREG specimens exhibit lower frequencies than the BFREG and CFREG. This is primarily due to the higher density of steel fibers with larger diameter and length than other fibers, which increases the mass of the composite and in result, reduces natural frequencies. The fiber addition enhances the stiffness, but the dominant effect of increased mass of SFREG reduces the natural frequencies. The close agreement (within ±5% variation) between the experimental and numerical values is observed across all modes. This validates the accuracy of the numerical model.

Table 11. Experimental and Numerical frequencies at various modes

BRFEG			
Mode	1st mode	3rd mode	6th mode
Experimental	52 Hz	282 Hz	492 Hz
Numerical	55.7 Hz	284.6Hz	493.3 Hz
CFREG			
Mode	1st mode	5th mode	6th mode
Experimental	58 Hz	322 Hz	558 Hz
Numerical	60.338 Hz	334.7 Hz	534.31 Hz
SFREG			
Mode	1st mode	4th mode	7th mode
Experimental	48 Hz	262 Hz	618 Hz
Numerical	47.312 Hz	262.62 Hz	640.23 Hz

4.4 Fibers' influence on the damping ratios

The computed damping ratios with mean values are presented in Table 12 and their comparison in Figure 15. The SFREG exhibits the highest damping values at the lower and middle ranges of frequencies compared to the BFREG and CFREG. This behavior is due to inherent properties of steel fibers, which enhance energy dissipation due to high density, internal friction, and more interfacial contact within the matrix. In the high frequency range, reduction of damping ratios of all composites is observed, which indicates that there is a decrease in energy dissipation capacity with increase in frequency. The frequencies and damping characteristics findings demonstrate that the dynamic behavior of the composites is strongly dependent on fiber characteristics viz. fiber type, fiber aspect ratio, fiber density, etc.

Table 12 Mean damping ratios

Composition	1	2	3	Mean damping ratio
BFERG	0.039	0.049	0.0156	0.035
CFREG	0.026	0.029	0.012	0.022
SFREG	0.052	0.053	0.04	0.048

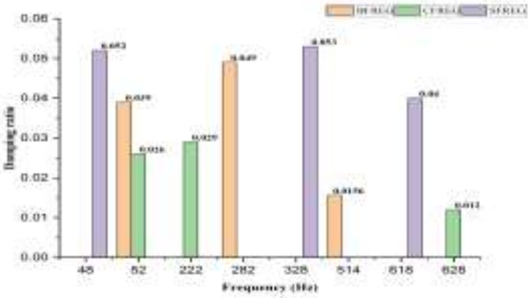

Fig. 15. Computed damping ratios at different frequencies

5. Conclusion

The study evaluates the influence of fiber addition on flexural and damping behaviour of epoxy granite. The results highlighted that fiber characteristics strongly influence the stiffness and damping capacities of epoxy granite composite. The developed composites demonstrate a prominent enhancement in vibration damping performance. The optimal balance between mass and stiffness is important for achieving the desired dynamic performance. The experimental and numerical results show close agreement, indicating the consistency and reliability of the numerical model. The epoxy granite provides a sustainable solution by recycling the granite waste produced. Therefore, fiber-added epoxy granite composites have significant potential for machine structure applications, viz. beds, bases, columns, etc.

Acknowledgments

The experimentation work was conducted at RIT, Islampur, Maharashtra, India.

Conflicts of Interest

There is no conflict of interest regarding the publication of this article.

References

[1] S. Orak, 2000. Investigation of vibration damping on polymer concrete with polyester resin, Cement and Concrete Research, 30, pp. 171–174.

[2] JML Reis, 2005. Mechanical Characterization of Fiber-reinforced Polymer Concrete. Materials Research, 8(3), pp. 357-360.

[3] Antonio Piratelli-Filho, Frank Shimabukuro, 2005. Characterization of Compression Strength of Granite-epoxy Composites Using Design of Experiments, Materials Research, 11(4), pp. 399-404.

[4] Fernando Cortés, G. Castillo, 2007. Comparison between the dynamical properties of polymer concrete and grey cast iron for machine tool applications, Materials & Design,28(5),pp.1461-66

[5] Wenfeng Bai, Jianhua Zhang, Peng Yan, Xinli Wang , 2009. Study on vibration alleviating properties of glass fiber-reinforced polymer concrete through orthogonal tests, Materials and Design, 30, pp.1417–1421.

[6] Antonio Piratelli Filho, Flaminio Levi Nito, 2010. Behavior of granite epoxy beams subjected to mechanical vibrations, Materials Research, 13(4), pp. 497-503.

[7] Sung-Kyum Cho, Hyun-Jun Kim, Seung-Hwan Chang, 2011. The application of polymer composites to the table-top machine tool components for higher stiffness and reduced weight, Composite Structures, 93, pp. 492–501.

[8] Joel Antony, D'Mello, S. S. Balakrishna, 2014. Assessment of Particulates Matrix Ratio and Its Influence on Mechanical Properties of Granite Particulates Reinforced Epoxy Composite, IJMET, 5(9), pp. 266-270.

[9] Subrahmanya Swamy. S , B. R. Sreedhar , Vinayak J. Kalas, Chandan K. M, 2014. Experimental Studies on Compression and Vibration Characteristics of Granite Epoxy- An Alternative Material for Precision Machine Tool Beds, IJPRET, 2 (10), pp. 120-135.

[10] S. S. Balakrishna, H. Girish, G. C. Mohan Kumar, S. Narendranath, 2014. Analysis on Mechanical and Dynamic behavior of Granite Epoxy Composites with Cast Iron Particulates as Filler, Indian Journal of Advances in Chemical Science, S1, pp.122-126.

[11] Francesco Aggogeri , Alberto Borboni, Angelo Merlo, Nicola Pellegrini, Raffaele Ricatto, 2017. Vibration Damping Analysis of Lightweight Structures in Machine Tools, Materials,10, pp.297.

[12]A. Vivek, Vijaya Holla, M.S. Krupashankara, A. Vignesh, Prasanna Kulkarni,2018. Effect Of Improving Damping Ratio On Surface Finish By Filling Particulate Reinforced Polymer Composites In Machine Tool Structures, MaterialsToday Proceedings, vol.5, issue 5, part 2,pp. 13664-13673.

[13] Joel D'Mello, Alister G D'Souza, Sushanth H Gowda, Denis Pinto, 2019. Experimental investigation of compression, flexural strength and damping behaviour of granite particulate epoxy matrix composite, AIP Conference Proceedings 2080; 020012. doi.org/10.1063/1.5092895

[14] Aditya Raj,Jayant Prakash Varun, P. K.,2019. Fabrication and Vibration Damping Analysis of Basalt Fiber-reinforced Composite Beam, AIP Conference Proceedings 2134;080002. doi.org/10.1063/1.5120242

[15] Huseyin Onur Ozturk, Yaşar Kahraman, 2019, Effects of glass fiber Reinforcement to Tensile Strength in Epoxy Matrix Granular Composite Materials, Sakarya University Journal of Science, 23(5), pp. 736-743.

[16]Jianwen Shao , Han Zhu , Xian Zuo , Wolong Lei , SaidMirgan Borito, Jian Liang, Fuqiang Dua n, 2020. Effect of waste rubber particles on the mechanical performance and deformation properties of epoxy concrete for repair, Construction and Building Materials, 241, pp.241.

[17] Mohamed Omar , Yasser Abdelrhman, Ibrahim M. Hassab, Wael M. Khierldeen, 2021. Experimental Study on Compressive Strength and Flexural Rigidity of Epoxy Granite Composite Material, Journal of Engineering Sciences Assiut University Faculty of Engineering, 49, pp. 198 – 214.

[18] Mohammed Y. Abdellah, Ahmed Abdelhaleem, Ibrahim A. Alnaser, G. T. Abdel-Jaber , Abdalla Abdal-hay,2021. Flexural, Compression and Fracture Properties of Epoxy Granite as a Cost-Effective Structure Materials, New Machine Element Foundation AIMS Materials Science, 8(1), pp. 82–98.

[19] Dr S. Nallusamy, Manikandan Narayanan, K. Sujatha and R. Suganthini Rekha,2021. Experimental Investigation of Mechanical Properties and Effect of Porosity on Epoxy Granite Composite, Material Science Forum 1042, pp.123-129.

[20] Yasser Abdelrhman , Mohamed Omar , Ibrahim M Hassab-Allah , W M Shewakh, Wael M Khierldeen, Mohammed Hedaya, Refaie Omar and Mohamed F Younes, 2024. Mechanical properties and damping characteristics of Egyptian granite-epoxy composite material, Material Research Express. 10.1088/2053-1591/ad4f5b

[21]Arif Ulu, 2024. Effect of resin amount on the damping properties of polymer concrete, Challenge Journal of concrete research letters,15(2), pp.47–55.

[22] Robert Wegner, Larissa Born, Michelle Engert, Kim T. Werkle, Hans-Christian Möhring & Götz T. Gresser,2025. Determination of the mechanical properties of prestressed fiber-reinforced polymer concrete, Materials and Structures, 58(291).

[23] Kailas V. Gurav,V. M. Kale, 2017. A review paper on Mechanical and Thermal Properties of Granite and its Industrial Applications, IJTARME, Volume -6, Issue-1-2 pp.76-81.

[24] ASTM E756-05, 2010, Standard Test Method for Measuring Vibration-Damping Properties of Materials (ASTM International).

[25] Araldite Epoxy Resin LY 556 With Hardener HY 951 technical data sheet.

[26] ASTM C78/C78M, 2021, Standard Test Method for Flexural Strength of Concrete (Using Simple Beam with Third-Point Loading)

[27] Montazeri, A., Rahmani, A. & Safarabadi, M., 2023. Performance and damage mechanism assessment of sandwich composites with glass/kenaf/epoxy skins and a novel core using quasi-static penetration. J Braz. Soc. Mech. Sci. Eng. 45, 256.

[28] Amin Montazeri, Iman Ahmadian, Ehsan Bahmanpour, Amirhossein Saeedi, Majid Safarabadi, 2025. Mechanical behaviors of star honeycombs with symmetry-broken lattices, European Journal of Mechanics - A/Solids, Volume 113.

[29] Arash Jafarpour, Majid Safarabadi Farahani, Mojtaba Haghighi-Yazdi, 2019. Numerical investigation of oriented CNFs effects on thermo-mechanical properties and curing residual stresses field of polymeric nanocomposites,Mechanics of Materials, Volume 138.